Aquaporin 4 Silencing Aggravates Hydrocephalus Induced by Injection of Autologous Blood in Rats

Authors' Contribution:
Study Design A
Data Collection B
Statistical Analysis C
Data Interpretation D
Manuscript Preparation E
Literature Search F
Funds Collection G

ABCDEF 1 Jian Guo
BCDEF 2 Xinjiang Mi
BCE 3 Rucai Zhan
BCD 1 Meng Li
BCD 1 Lin Wei
AE 1 Jinlong Sun

1 First Department of Neurosurgery, Shandong Provincial Qianfoshan Hospital, Shandong University, Jinan, Shandong, P.R. China
2 Second Department of Surgery, Shandong Police Hospital, Jinan, Shandong, P.R. China
3 Second Department of Neurosurgery, Shandong Provincial Qianfoshan Hospital, Shandong University, Jinan, Shandong, P.R. China

Corresponding Author: Jinlong Sun, e-mail: 13805311206@163.com
Source of support: This study was supported by the Science and Technology Development Project of Shandong Province under grant number 2010GSF10211

Background: Aquaporin 4 (AQP4), the most abundant aquaporin in the brain, is a type of bidirectional water channel controlling the brain-water balance and plays a critical role in physiologic and pathologic water balance in the brain. AQP4 was reported to be elevated in hydrocephalus; therefore, we hypothesized that AQP4 contributes to hydrocephalus. In this study, the role of AQP4 in hydrocephalus was explored.

Material/Methods: The hydrocephalus rat model was established by injection of autologous blood. On Day 1 and Day 3 after injection of autologous blood, magnetic resonance imaging (MRI) and hematoxylin-eosin (HE) staining were performed to detect the changes in ventricles, and quantitative real-time PCR (qRT-PCR) and immunohistochemistry were carried out to detect the changes in AQP4 level. Thereafter, an AQP4-specific siRNA was used to downregulate AQP4. Then, on Day 3 after injection of autologous blood, the levels of AQP4 and connexin-43 were detected by qRT-PCR, immunohistochemistry, immunofluorescence, or Western blot analysis. MRI and HE staining were performed to detect the changes in ventricles, and Evans blue extravasation assay was used to assess blood-brain barrier integrity.

Results: The hydrocephalus rat model was established successfully, and hydrocephalus rats showed a higher AQP4 level. Silencing AQP4 aggravated the hydrocephalus, with enlarged lateral ventricles and destruction of ependymal integrity and blood-brain barrier.

Conclusions: Our study demonstrates that silencing AQP4 aggravates hydrocephalus, indicating that AQP4 protects against hydrocephalus.

MeSH Keywords: Aquaporin 4 • Blood-Brain Barrier • Ependyma • Hydrocephalus

Full-text PDF: https://www.medscimonit.com/abstract/index/idArt/906936

📄 3048   ▦ —   📊 7   📑 25

Background

Hydrocephalus is a central nervous system disorder that is commonly due to an imbalance between cerebrospinal fluid production and absorption. Excessive accumulation of cerebrospinal fluid leads to ventriculomegaly, increased intracranial pressure, and impaired neuronal functions [1]. At present, shunting is the main therapeutic method for treating hydrocephalus, but it has a high failure rate.

Aquaporins are a family of bidirectional water channel proteins expressed in plasma membranes. There are at least 13 aquaporins discovered in mammals [2]. Aquaporins in the brain have 3 major functions: brain-water balance, cell migration, and neural signal transduction [3].

Aquaporin 4 (AQP4) is the most abundant aquaporin in the brain [4]. It is expressed mainly in the foot processes of pericapillary astrocytes at the blood-brain border and brain-cerebrospinal fluid border, and controls the movement of water in the brain [3–5]. AQP4 plays a critical role in physiologic and pathologic water balance in the brain [4,6], and is reported to be associated with the pathology of brain edema, which is a disease caused by brain-water imbalance [2,4,7–10].

As hydrocephalus is a disease strongly related to defects in cerebrospinal fluid circulation, regulating water channels may become a promising therapeutic approach. The level of AQP4 was found to be elevated in subjects with hydrocephalus [11–13]; therefore, we hypothesized that AQP4 contributes to the pathology of hydrocephalus. In the present study, the role of AQP4 in hydrocephalus was explored in a rat model of hydrocephalus established by injection of autologous blood.

Material and Methods

Animals

Healthy SD rats (male, 12 weeks old, 260–300 g) were obtained from Liaoning Changsheng biotechnology Co., Ltd (Shenyang, China). Rats were raised in standard conditions (temperature 23±1°C, relative humidity 50±5%, 12 h/12 h light/dark cycles) and had *ad libitum* access to standard laboratory chow and water. This study was performed in accordance with the *Guide for Care and Use of Laboratory Animals* and was approved by the Laboratory Animal Welfare and Ethics Committee of Shandong University.

Experimental protocol

This study included 2 parts. Random grouping was carried out. In Part I, rats in the hydrocephalus group (n=12) received injection of autologous blood to establish a hydrocephalus model. Briefly, rats were anesthetized with pentobarbital sodium (50 mg/kg, intraperitoneal injection). A cranial burr hole (1 mm) was drilled, and 200 ul non-heparinized autologous blood was injected into the ventricle (coordinates: 0.6 mm posterior, 1.6 mm lateral, 4.5 mm ventral to the bregma) using a microinfusion pump. After injection, the microinfusion pump was removed, and the wound was closed. Rats in the control group (n=12) received injection of an equal volume of saline into the ventricle. On Day 1 and Day 3 after injection of autologous blood or saline, magnetic resonance imaging (MRI) scanning was performed to determine lateral ventricle enlargement. Rats were sacrificed after MRI, and their brain tissues were obtained for subsequent hematoxylin-eosin (HE) staining, immunohistochemistry analysis, and quantitative real-time PCR (qRT-PCR) (n=6 for each time point).

Part II included 3 groups: the AQP4 siRNA group, the negative control of siRNA group, and the control group (n=18 for each group). The experimental procedure is shown in Figure 1. We mixed 400 ng AQP4 siRNA (GenePharma, Shanghai, China) with 2 μl Interferin transfection reagent (Polyplus-transfection, Illkirch, France) and injected the mixture into the lateral ventricle of rats in the AQP4 siRNA group. Twenty-four hours later, these rats received injection of autologous blood. The second injection of AQP4 siRNA (400 ng; mixed with 2 μl Interferin) was performed at 24 h after injection of autologous blood. Rats in the negative control of siRNA group received injection of autologous blood and 2 injections of negative control of siRNA (GenePharma, 400 ng mixed with 2 μl Interferin, at 24 h before and 24 h after injection of autologous blood). Rats in the control group received injection of normal saline. On Day 3 after injection of autologous blood or saline, MRI scanning and Evans blue extravasation assay were carried out. Then, the rats were sacrificed and their brain tissues were obtained for subsequent qRT-PCR, Western blot, immunohistochemistry, immunofluorescence, and HE staining (n=6 for each experiment).

MRI scanning

MRI was performed on Day 1 and Day 3 after injection of autologous blood in a 3.0-T Varian MR Scanner (Siemens Healthcare, Forchheim, Germany). T2-weighted imaging and 1-mm–thick continuous coronal section images of rats in each group were obtained (TR/TE=5000/86 ms). Images were analyzed using Image-pro Plus 6.0 software. The lateral ventricle volume was calculated by summing the lateral ventricle areas over all slices and multiplying by the thickness of sections.

Evans blue extravasation assay

We injected 2% Evans blue dye into rats (2 ml/kg) through a tail vein. Two hours later, the rats were sacrificed and perfused
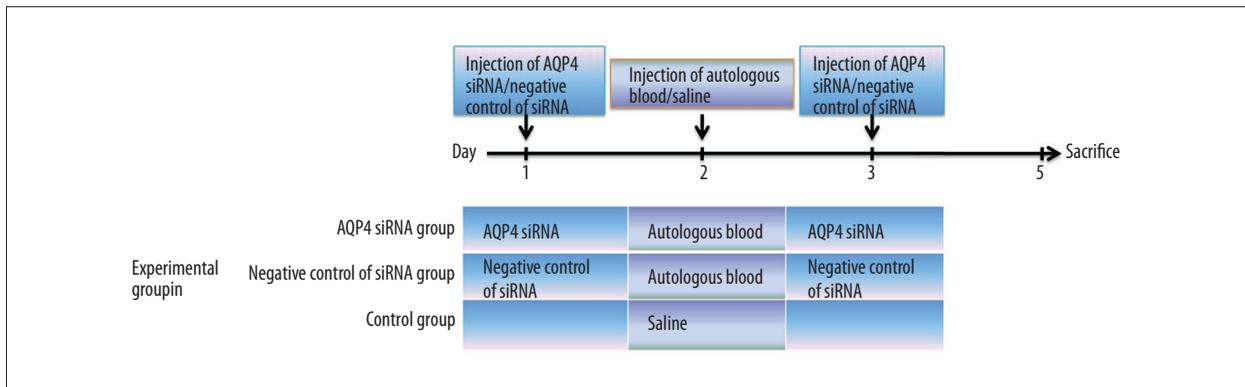
Figure 1. Experimental procedure of injection of autologous blood and siRNA in experiment Part II.

with saline via the left ventricle until colorless perfusion fluid appeared. Then, brain tissues were harvested, homogenized in formamide (1 ml formamide/100 g brain tissues), and incubated at 37C for 24 h to extract Evans blue dye. After centrifugation, the absorbance of supernate was measured at 632 nm, and the content of Evans blue dye was calculated.

HE staining

Brain tissues of rats in each group were obtained, fixed in 10% formalin, embedded in paraffin, and cut into 5-μm slices. The slices were deparaffinized in xylene, rehydrated in gradient ethanol, and then stained with hematoxylin and eosin. Images were captured using a light microscope (OLYMPUS, Tokyo, Japan) with a 200× magnification.

Immunohistochemistry

The paraffin-embedded brain tissues were cut into 5-μm slices. After being deparaffinized and rehydrated, the slices were subjected to retrieve antigen in antigen retrieval buffer for 10 min. Then, the slices were incubated with 3% H_2O_2 for 15 min to quench the activity of endogenous peroxidases, and incubated with goat serum (Solarbio, Beijing, China) for 15 min at room temperature to block non-specific binding. Thereafter, the slices were incubated with AQP4 antibodies (rabbit anti-AQP4 antibody; 1: 50 diluted in PBS; Proteintech, Wuhan, China) or Connexin 43 antibody (rabbit anti-connexin 43 autoantibody; 1: 50 diluted in PBS; Proteintech) overnight at 4°C. The slices were rinsed in PBS and incubated with corresponding secondary antibodies (biotin-conjugated goat anti-rabbit IgG; 1: 200 diluted in PBS; Beyotime, Shanghai, China) for 30 min at 37°C. The slices were rinsed in PBS, incubated with horseradish peroxidase (HRP)-conjugated avidin (Beyotime) for 30 min at 37°C, and visualized using a DAB (3, 3'-diaminobenzidine) Kit (Solarbio). Next, the slices were counterstained with hematoxylin (Solarbio) and observed using a light microscope with a 400× magnification.

Immunofluorescence

After being deparaffinized and rehydrated, the slices were antigen-retrieved in antigen retrieval buffer and blocked with goat serum. Then, the slices were incubated with AQP4 antibody (rabbit anti-AQP4 antibody; 1: 50 diluted in PBS; Proteintech) and glial fibrillary acidic protein (GFAP) antibody (mouse anti-GFAP antibody; 1: 50 diluted in PBS; Santa Cruz, Dallas, TX, USA) overnight at 4°C. After being rinsed in PBS, the slices were incubated with corresponding secondary antibodies (Cy3-conjugated goat anti-rabbit IgG, FITC-conjugated goat anti-mouse IgG; 1: 200 diluted in PBS; Beyotime) for 90 min at room temperature in the dark. Thereafter, the slices were rinsed in PBS and incubated with DAPI (4',6-diamidino-2-phenylindole) (Beyotime) for nuclear counterstaining. The slices were observed using a fluorescence microscope (OLYMPUS; model: BX53) with a 400× magnification.

QRT-PCR

Total RNA in brain tissues was extracted using the High-purity Total RNA Fast Extraction Kit (BioTeke, Beijing, China) according to the manufacturer's instructions. Then, the RNA was reversely transcribed to cDNA with oligo(dT)$_{15}$ and M-MLV reverse transcriptase (BioTeke) according to the protocol. The mRNA levels of AQP4 were determined using qRT-PCR on an Exicycler™ 96 real-time quantitative thermal block (BIONEER, Daejeon, Korea). The following primers were used: AQP4 forward primer: 5'-ATCGCCAAGTCCGTCTTCTACATC-3'; AQP4 reverse primer: 5'-AACCGTGGTGACTCCCAATCC-3'; β-actin forward primer: 5'-GGAGATTACTGCCCTGGCTCCTAGC-3'; β-actin reverse primer: 5'-GGCCGGACTCATCGTACTCCTGCTT-3'. The SYBR Green reagent was obtained from Solarbio. The mRNA level of AQP4 was normalized to β-actin and calculated using $2^{-\Delta\Delta Ct}$ method.

Western blot analysis

Brain tissues were homogenized on ice in Radioimmuno-precipitation Assay Lysis Buffer (Beyotime) containing 1%
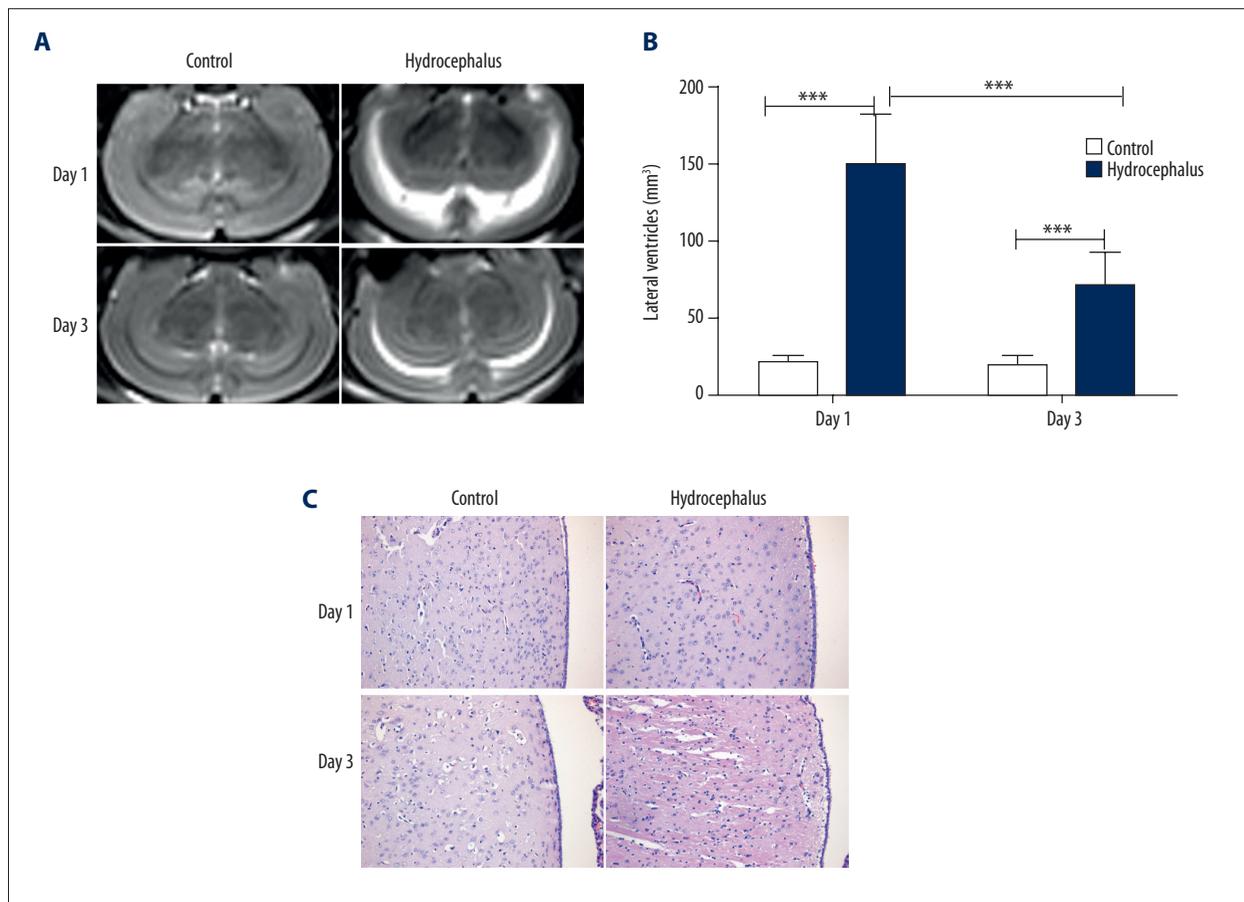
Figure 2. Injection of autologous blood induced hydrocephalus. (**A**) Ventricles of rats in each group were observed using magnetic resonance imaging (n=6). (**B**) The lateral ventricular volumes of rats in each group were calculated. (**C**) The brain tissues of rats in each group were detected through hematoxylin-eosin staining (n=6). Typical images are presented. The results are presented as mean ± SD. *** p<0.001.

phenyl-methane-sulfonyl fluoride (Beyotime). After centrifugation at 10005×g for 10 min at 4°C, the protein concentration of supernatant was measured with a BCA Protein Assay Kit (Beyotime). Thereafter, 40 µg proteins from each group were separated by 10% sodium dodecyl sulfate-polyacrylamide gel electrophoresis and then transferred onto polyvinylidene fluoride membranes (Millipore, Bedford, MA, USA). The membranes were blocked with 5% non-fat milk, rinsed in Tris-buffered saline with Tween (TBST), and incubated with AQP4 antibody (rabbit anti-AQP4 antibody; 1: 500 diluted; Proteintech), connexin 43 antibody (rabbit anti-connexin 43 antibody; 1: 500 diluted; Proteintech), or β-actin antibody (mouse anti-β-Actin antibody; 1: 500 diluted; Bioss, Beijing, China) overnight at 4°C. Thereafter, the membranes were rinsed in TBST and incubated with corresponding HRP-conjugated secondary antibodies (goat anti-rabbit IgG, goat anti-mouse IgG; 1: 5000 diluted; Beyotime) for 45 min at 37°C. The membranes were visualized using an Enhanced Chemiluminescence Kit (Beyotime), followed by chemiluminescence detection on X-ray film. β-actin was applied as the internal control. The intensities of targeted bands were analyzed with Gel-Pro-Analyzer software.

Statistical analysis

The results are presented as mean ±SD. Differences between groups were analyzed using one-way Analysis of Variance (ANOVA) or two-way ANOVA followed by Bonferroni post hoc testing. P<0.05 was considered as significant.

Results

Injection of autologous blood induced hydrocephalus

After injection of autologous blood, the brain tissues of rats in each group were determined by MRI, and the lateral ventricle volumes were calculated. As shown in Figure 2, after injection of autologous blood, ventriculomegaly was discovered on Day 1 (Figure 2A), with significantly increased lateral ventricle volumes (Figure 2B). The ventriculomegaly on Day 3 after injection of autologous blood was also remarkable, with significantly increased lateral ventricle volumes, but was less
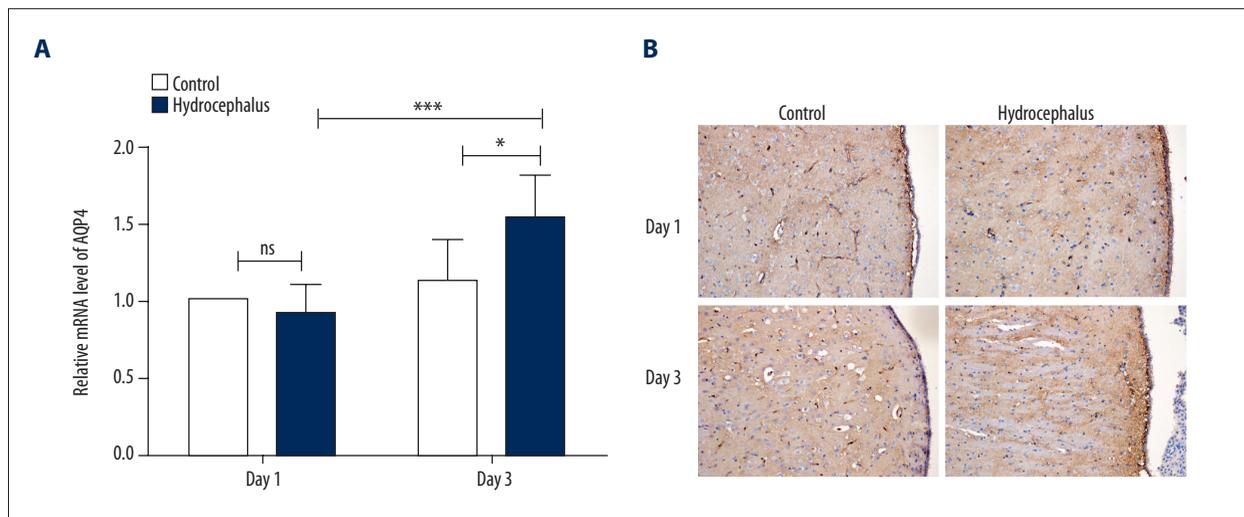
Figure 3. AQP4 level was increased in hydrocephalus models. (**A**) The mRNA level of AQP4 in the brain tissues of rats in each group was measured by quantitative real-time PCR (n=6). The mRNA level of AQP4 was normalized to β-actin and calculated using $2^{-\Delta\Delta Ct}$ method. (**B**) Immunohistochemistry was used to detect the expression of AQP4 in the brain tissues of rats in each group (n=6). The results are presented as mean ±SD and typical results are presented. * p<0.05; *** p<0.001; ns – no significance.

pronounced than those on Day 1 (Figure 2A, 2B). On Day 3, disorganization in ependymal layer was observed, as detected by HE staining (Figure 2C). These results demonstrated that injection of autologous blood can effectively induce hydrocephalus.

The AQP4 level was elevated in hydrocephalus model

After induction of hydrocephalus by injection of autologous blood, the level of AQP4 in brain tissues was detected by qRT-PCR and immunohistochemistry. As shown in Figure 3A, the AQP4 level in the control group showed no significant difference between Day 1 and Day 3. On the first day after hydrocephalus induction, the AQP4 level in the hydrocephalus group showed a slight but not significant decrease compared with the control group. However, on Day 3, the level of AQP4 in the hydrocephalus group was significantly higher than that in the control group (Figure 3A, p< 0.05). The expression and distribution of AQP4 were also detected by immunohistochemistry. On Day 3, the expression of AQP4 in the hydrocephalus group was increased compared with the control group, especially in the ependymal layer (Figure 3B). These results indicated that the AQP4 level in the hydrocephalus model was elevated.

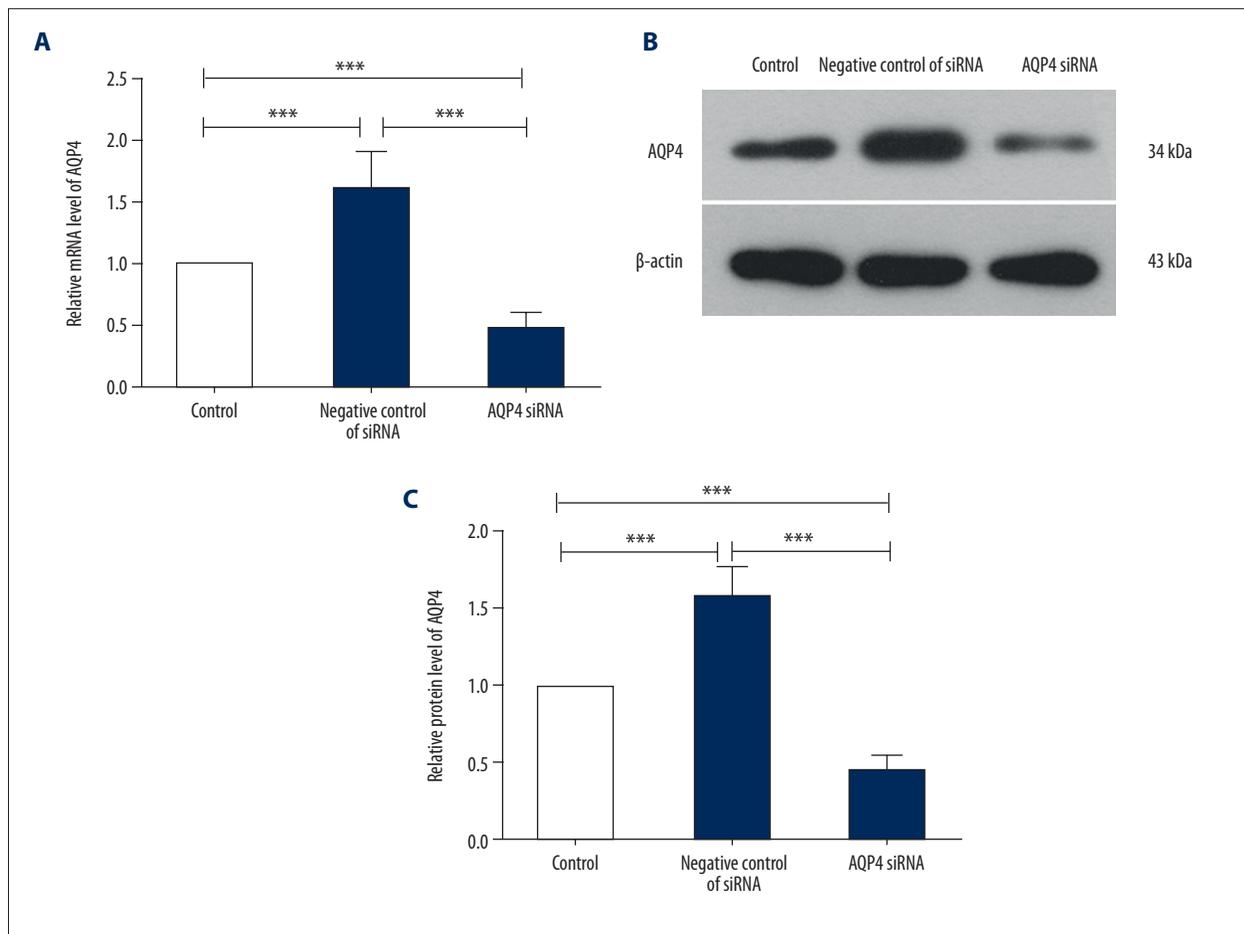**AQP4 siRNA decreased the AQP4 level in brain tissues**

According to our previous results, an AQP4-specific siRNA was employed to explore the role of AQP4 in hydrocephalus. First, the efficiency of AQP4 siRNA was verified by qRT-PCR and Western blot analysis. The results of qRT-PCR analysis showed that, after hydrocephalus induction and transfection with negative control of siRNA, the relative mRNA level of AQP4 was

increased to 1.61±0.31. However, AQP4 siRNA decreased the relative mRNA level of AQP4 to 0.46±0.13 (Figure 4A). The results of Western blot analysis also showed that, compared with the negative control of siRNA group, the protein level of AQP4 was decreased by AQP4 siRNA (Figure 4B, 4C). The expression and distribution of AQP4 and its co-localization with GFAP, a marker of astrocytes, was detected by immunofluorescence. As shown in Figure 5, AQP4 was co-localized with GFAP in hydrocephalus brains. After AQP4 silencing, the AQP4 level was decreased, especially that co-localized with GFAP in the ependymal layer. These results demonstrate that AQP4 siRNA can efficiently decrease the AQP4 level.

AQP4 siRNA aggravated hydrocephalus

After AQP4 silencing, the brains of rats in each group were assessed by MRI. In the negative control of siRNA group, injection of autologous blood caused hydrocephalus, which was consistent with our previous results. When AQP4 was silenced, the hydrocephalus was aggravated, and the lateral ventricle volumes were increased significantly compared with the negative control of siRNA group (Figure 6A, 6B, p<0.01). Moreover, the brain tissues were assessed by HE staining, showing that the disorganized ependymal layer induced by hydrocephalus was aggravated by AQP4 silencing (Figure 6C).

The expression and distribution of connexin 43, a gap junction protein, was also detected by Western blot and immunohistochemistry. As shown in Figure 7, the protein level of connexin 43 in the negative control of siRNA group was increased after injection of autologous blood. However, in the AQP4 siRNA group,

Figure 4. AQP4 siRNA decreased the AQP4 level in rat brain tissues. (**A**) Quantitative real-time PCR was used to detect the mRNA level of AQP4 in rat brain tissues in each group (n=6). The mRNA level of AQP4 was normalized to β-actin and calculated using $2^{-\Delta\Delta Ct}$ method. (**B**) The protein level of AQP4 in the rat brain tissues was detected by western blot with β-actin as the internal control (n=6). (**C**) The relative protein level of AQP4 in each group was calculated. The results are shown as mean ±SD. *** p<0.001.

this increase was reduced by AQP4 silencing (Figure 7A, 7B). The results of immunohistochemistry showed similar results: the increased connexin 43 level in ependymal layer induced by hydrocephalus was reduced by AQP4 silencing (Figure 7C).

The integrity of the blood-brain barrier was also assessed in our study through Evans blue extravasation assay. The Evans blue content in the negative control of siRNA group was increased compared with the control group, indicating that the blood-brain barrier was damaged. In the AQP4 siRNA group, the Evans blue content was higher than in the negative control of siRNA group (Figure 7D), indicating that the damaged blood-brain barrier in hydrocephalus brains was aggravated by AQP4 silencing.

Discussion

The literature shows that brain-water homeostasis is very important to hydrocephalus. In the present study, the role of AQP4 in hydrocephalus was explored. The results of our study showed that the AQP4 level was elevated after induction of hydrocephalus. However, silencing AQP4 aggravated hydrocephalus and impaired blood-brain barrier and ependymal integrity. Our results suggest that AQP4 has a protective effect during hydrocephalus.

AQP4, a water channel protein, is mainly expressed in astrocyte end-feet processes and glia limitans. It has a close relationship with brain water homeostasis and facilitates the transport of excess water out of the brain. Periventricular AQP4 level is reported to be positively correlated to cerebrospinal fluid volume [14]. AQP4 deficiency can lead to increased water accumulation in the central nervous system, as well as brain swelling
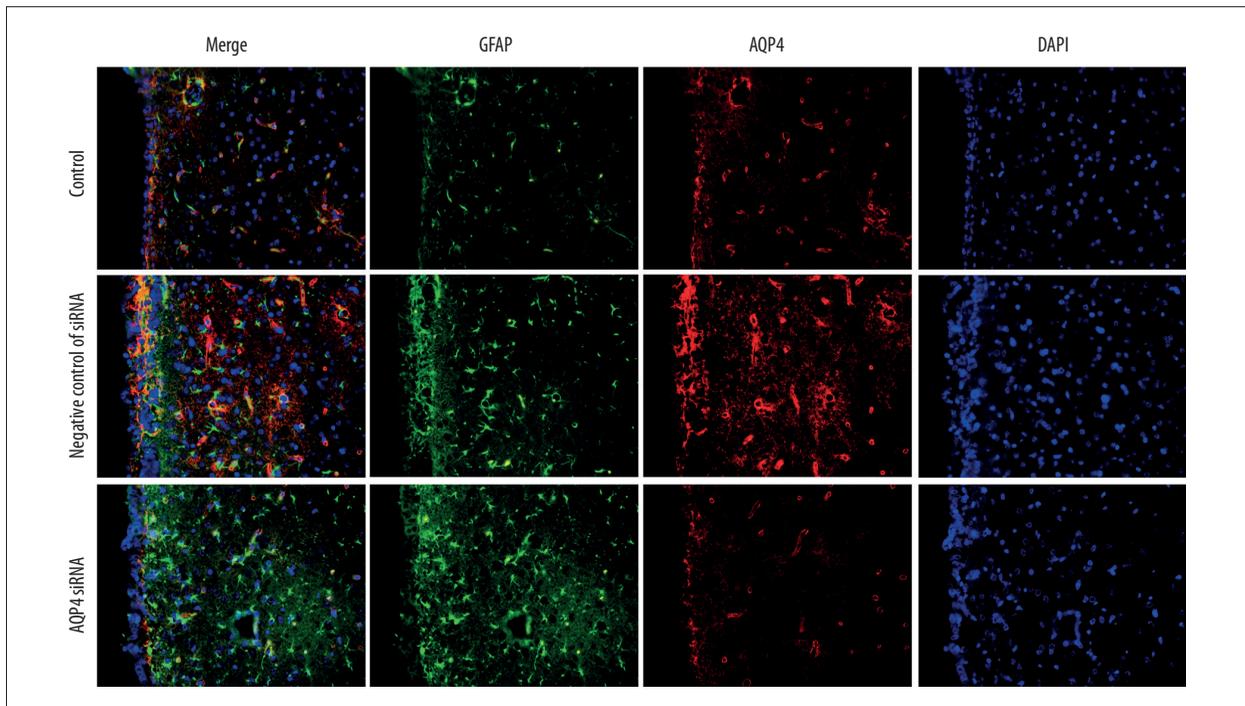
Figure 5. AQP4 siRNA influenced the expression and distribution of AQP4. Immunofluorescence was used to detect the expression and distribution of GFAP and AQP4 (n=6). Green fluorescence: GFAP; red fluorescence: AQP4; blue fluorescence: DAPI.
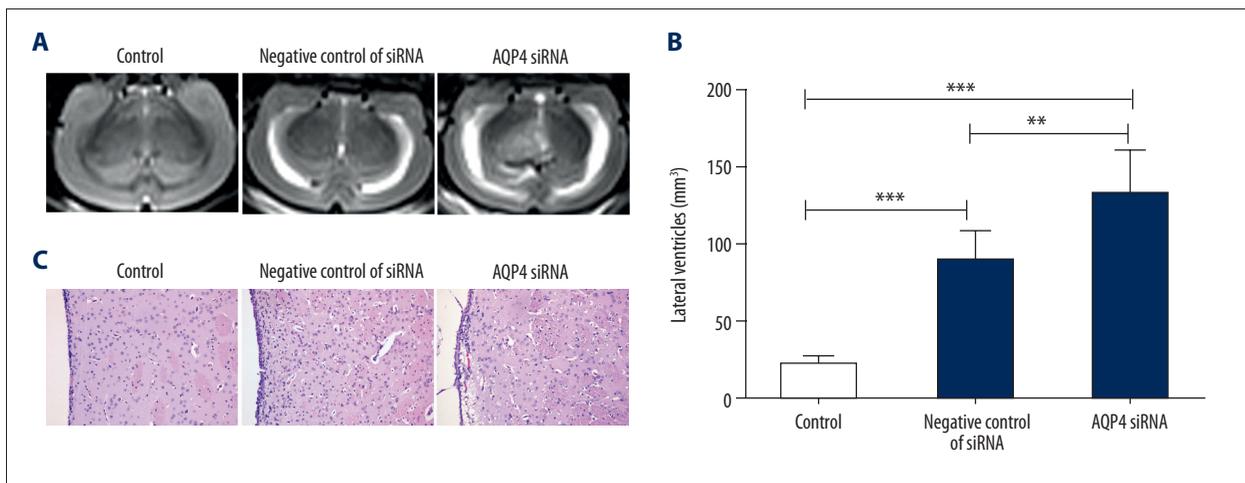

Figure 6. Silencing AQP4 aggravated hydrocephalus. (**A**) After silencing AQP4, the brains of rats in each group were checked using magnetic resonance imaging (n=6). (**B**) The lateral ventricular volumes of rats in each group. (**C**) Hematoxylin-eosin staining was used to detect the brain tissues of rats in each group (n=6). The results are shown as mean ±SD. ** $p<0.01$; *** $p<0.001$.

or deteriorated neurological outcomes [15]. The AQP4 level was reported to be elevated in rat models of hydrocephalus induced by injection of kaolin [11], as well as in hydrocephalus dogs [12]. Consistently, our study found that the AQP4 level was also elevated in rat hydrocephalus models induced by injection of autologous blood. Moreover, in congenital hydrocephalus patients, the cerebrospinal fluid also shows a higher AQP4 expression [13]. A variety of studies show that the AQP4 level in cerebrospinal fluid and parenchyma of subjects

with hydrocephalus is elevated, and this disturbance is correlated with hydrocephalus severity [13,14,16]. This suggests that AQP4 has a relationship with hydrocephalus.

AQP4 can facilitate water passing from ventricles into brain parenchyma and then to the systemic circulation [1]. Whether the disturbance in AQP4 is contributes to hydrocephalus or is protective remains unclear. We first thought that the disturbance of AQP4 might contribute to hydrocephalus. However,
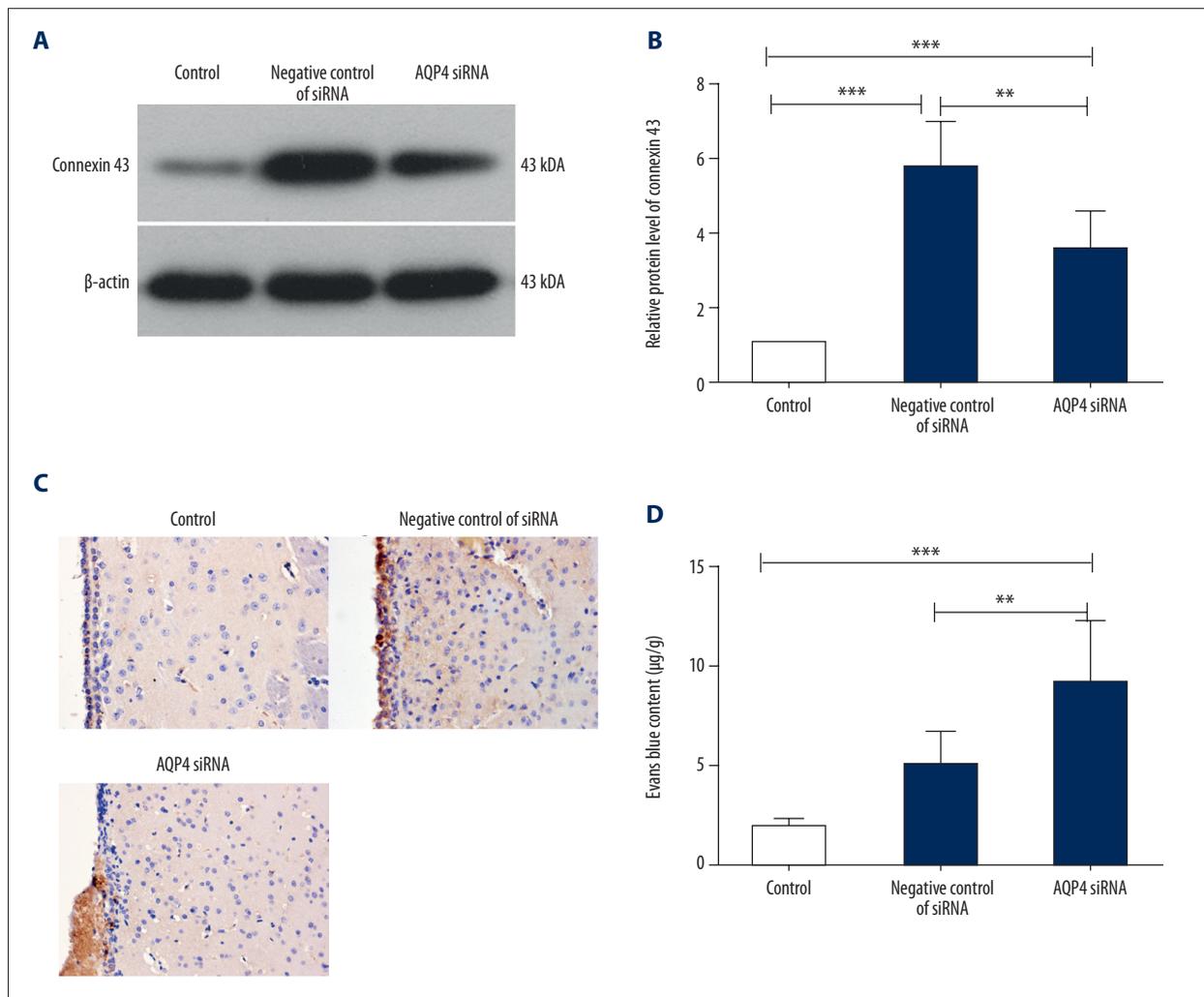
Figure 7. AQP4 silencing impacted the integrity of ependyma and blood-brain barrier. (**A**) Western blot was performed to detect the protein level of connexin 43 in the brain tissues in each group (n=6). (**B**) The relative protein level of connexin 43 was calculated with β-actin as the internal control. (**C**) The protein level of connexin 43 in the brain tissues was detected by immunohistochemistry (n=6). (**D**) Evans blue extravasation was carried out to detect the integrity of the blood-brain barrier (n=6). Typical images are presented. The results are shown as mean ±SD. ** $p<0.01$; *** $p<0.001$.

in the present study, we found that the severity of hydrocephalus on Day 3 was less than on Day 1, whereas, the AQP4 level was higher. This result suggests that AQP4 has a protective role in hydrocephalus. If the disturbance of AQP4 contributes to hydrocephalus, AQP4 silencing would result in alleviation. On the contrary, if the disturbance of AQP4 protects against hydrocephalus, AQP4 silencing would result in aggravation. We found that AQP4 silencing resulted in aggravated hydrocephalus. Consistent with our results, in kaolin-induced hydrocephalus, AQP-4 null mice showed a more severe hydrocephalus [17]; and in obstructive hydrocephalus, AQP4 knockout increased the ventricular enlargement, and its deficiency accelerates the hydrocephalus progression [17]. Thus, we hypothesize that AQP4 protects against hydrocephalus. Some researchers also consider that the disturbance of AQP4 is an adaptive

response to hydrocephalus, and has a compensatory effect in altering the pathway of cerebrospinal fluid absorption [12,14]. However, to verify this hypothesis, more research is needed.

AQP4 plays a complicated role in diseases associated with water imbalance in the brain. In cytotoxic brain edema, in which water is accumulated in intracellular compartments, AQP4 provides an important route for water to move into the brain. AQP4 knockout can attenuate brain edema [18], and AQP4 overexpression can accelerate brain edema [19]. On the contrary, in vasogenic brain edema, in which water is accumulated in interstitial spaces, AQP4 removes excess water, and AQP4 knockout can aggravate the brain edema [20]. In the present study, AQP4 silencing aggravated hydrocephalus, which is characterized by excessive cerebrospinal fluid accumulation. These

different roles of AQP4 in cytotoxic brain edema, vasogenic brain edema, and hydrocephalus may be due to the different sites where water is accumulated. However, more evidence is needed to verify this hypothesis.

Ependyma and blood-brain barrier are the barriers between intracerebral fluid and brain parenchyma. AQP4 is a bidirectional water channel strongly present in astroglia at the blood-brain barrier and cerebrospinal fluid-brain interfaces [4,21]. Thus, AQP4 may play an important role in brain-water homeostasis. Connexin 43 is the main gap junction protein expressed in ependymal cells and astrocytes [22,23]. In our study, the level of connexin 43 was elevated after induction of hydrocephalus, but was reduced by AQP4 silencing. Consistently, Li et al. and Nicchia et al. also showed that AQP4 deficiency or knockdown decreased the level of connexin 43 [24,25]. These results suggest that AQP4 silencing also affects the gap junction between ependymal cells, thus altering ependymal integrity. Moreover, the impaired blood-brain barrier integrity was also exacerbated by AQP4 silencing. As blood-brain barrier and ependymal integrity are related to brain-water homeostasis, the role of AQP4 in hydrocephalus may be associated with its effects on blood-brain barrier and ependymal integrity.

Conclusions

In our study, a rat model of hydrocephalus showed a higher AQP4 level. Moreover, silencing AQP4 was found to aggravate the hydrocephalus. It seems that AQP4 performs a protective role against hydrocephalus. Modulating AQP4 may be an attractive therapy for the treatment of hydrocephalus. Given that AQP4 performs different roles in different types of brain edema, the role of AQP4 in hydrocephalus may differ depending on the types of hydrocephalus. To verify the exact role of AQP4 in hydrocephalus, more explorations are needed.

Acknowledgements

Conflict of interest

None.

References:

1. Aghayev K, Bal E, Rahimli T et al: Aquaporin-4 expression is not elevated in mild hydrocephalus. Acta Neurochir (Wien), 2012; 154: 753–59

2. Papadopoulos MC, Verkman AS: Aquaporin-4 and brain edema. Pediatr Nephrol, 2007; 22: 778–84

3. Papadopoulos MC, Verkman AS: Potential utility of aquaporin modulators for therapy of brain disorders. Prog Brain Res, 2008; 170: 589–601

4. Badaut J, Lasbennes F, Magistretti PJ, Regli L: Aquaporins in brain: Distribution, physiology, and pathophysiology. J Cereb Blood Flow Metab, 2002; 22: 367–78

5. Nico B, Frigeri A, Nicchia GP et al: Role of aquaporin-4 water channel in the development and integrity of the blood-brain barrier. J Cell Sci, 2001; 114: 1297–307

6. Bloch O, Papadopoulos MC, Manley GT, Verkman AS: Aquaporin-4 gene deletion in mice increases focal edema associated with staphylococcal brain abscess. J Neurochem, 2005; 95: 254–62

7. Taniguchi M, Yamashita T, Kumura E et al: Induction of aquaporin-4 water channel mRNA after focal cerebral ischemia in rat. Brain Res Mol Brain Res, 2000; 78: 131–37

8. Xu M, Su W, Xu QP: Aquaporin-4 and traumatic brain edema. Chin J Traumatol, 2010; 13: 103–10

9. Katada R, Nishitani Y, Honmou O et al: Expression of aquaporin-4 augments cytotoxic brain edema after traumatic brain injury during acute ethanol exposure. Am J Pathol, 2012; 180: 17–23

10. Chu H, Huang C, Ding H et al: Aquaporin-4 and cerebrovascular diseases. Int J Mol Sci, 2016; 17: 1249

11. Mao X, Enno TL, Del Bigio MR: Aquaporin 4 changes in rat brain with severe hydrocephalus. Eur J Neurosci, 2006; 23: 2929–36

12. Schmidt MJ, Rummel C, Hauer J et al: Increased CSF aquaporin-4, and interleukin-6 levels in dogs with idiopathic communicating internal hydrocephalus and a decrease after ventriculo-peritoneal shunting. Fluids Barriers CNS, 2016; 13: 12

13. Castaneyra-Ruiz L, Gonzalez-Marrero I, Gonzalez-Toledo JM et al: Aquaporin-4 expression in the cerebrospinal fluid in congenital human hydrocephalus. Fluids Barriers CNS, 2013; 10: 18

14. Tourdias T, Dragonu I, Fushimi Y et al: Aquaporin 4 correlates with apparent diffusion coefficient and hydrocephalus severity in the rat brain: A combined MRI-histological study. Neuroimage, 2009; 47: 659–66

15. Verkman AS, Binder DK, Bloch O, Auguste K, Papadopoulos MC: Three distinct roles of aquaporin-4 in brain function revealed by knockout mice. Biochim Biophys Acta, 2006; 1758: 1085–93

16. Desai B, Hsu Y, Schneller B et al: Hydrocephalus: the role of cerebral aquaporin-4 channels and computational modeling considerations of cerebrospinal fluid. Neurosurg Focus, 2016; 41: E8

17. Bloch O, Auguste KI, Manley GT, Verkman AS: Accelerated progression of kaolin-induced hydrocephalus in aquaporin-4-deficient mice. J Cereb Blood Flow Metab, 2006; 26: 1527–37

18. Manley GT, Fujimura M, Ma T et al: Aquaporin-4 deletion in mice reduces brain edema after acute water intoxication and ischemic stroke. Nat Med, 2000; 6: 159–63

19. Yang B, Zador Z, Verkman AS: Glial cell aquaporin-4 overexpression in transgenic mice accelerates cytotoxic brain swelling. J Biol Chem, 2008; 283: 15280–86

20. Papadopoulos MC, Manley GT, Krishna S, Verkman AS: Aquaporin-4 facilitates reabsorption of excess fluid in vasogenic brain edema. FASEB J, 2004; 18: 1291–93

21. Amiry-Moghaddam M, Otsuka T, Hurn PD et al: An alpha-syntrophin-dependent pool of AQP4 in astroglial end-feet confers bidirectional water flow between blood and brain. Proc Natl Acad Sci USA, 2003; 100: 2106–11

22. Rash JE, Yasumura T, Davidson KG et al: Identification of cells expressing Cx43, Cx30, Cx26, Cx32 and Cx36 in gap junctions of rat brain and spinal cord. Cell Commun Adhes, 2001; 8: 315–20

23. Chanson M, Kotsias BA, Peracchia C, O'Grady SM: Interactions of connexins with other membrane channels and transporters. Prog Biophys Mol Biol, 2007; 94: 233–44

24. Li X, Kong H, Wu W et al: Aquaporin-4 maintains ependymal integrity in adult mice. Neuroscience, 2009; 162: 67–77

25. Nicchia GP, Srinivas M, Li W et al: New possible roles for aquaporin-4 in astrocytes: Cell cytoskeleton and functional relationship with connexin43. FASEB J, 2005; 19: 1674–76